Biochemical and Biophysical Research Communications **287,** 277–281 (2001)
doi:10.1006/bbrc.2001.5555, available online at http://www.idealibrary.com on IDEAL®

Molecular Model for the Binary Complex of Uropepsin and Pepstatin

Walter F. de Azevedo Jr.,*,†,[1] Fernanda Canduri,*,† Valmir Fadel,*,†
Lívia G. V. L. Teodoro,‡ Valdemar Hial,‡ and Roseli A. S. Gomes‡
**Departamento de Física, IBILCE, UNESP, São José do Rio Preto, SP 15054-000, Brazil; †Center for Applied Toxinology, Instituto Butantan, Av. Vital Brazil, 1500, São Paulo, SP 05503-900, Brazil; and ‡Departamento de Ciências Biológicas, FMTM, Uberaba, MG 38015-050, Brazil*

Received July 11, 2001

The three-dimensional structure of human uropepsin complexed with pepstatin has been modelled using human pepsin as a template. Uropepsin is an aspartic proteinase from the urine, produced in the form of pepsinogen A in the gastric mucosa. The structure is bilobal, consisting of two predominantly β-sheet lobes which, as observed in other aspartic proteinases, are related by a pseudo twofold axis. A structural comparison between binary complexes of pepsin:pepstatin and uropepsin:pepstatin is discussed.

Key Words: **aspartic proteinase; uropepsin; pepstatin; complex; model; structure.**

Aspartic proteinases (EC 3.4.23) from one class of proteolytic enzymes that can be found in different organisms, ranging from humans to plants and retroviruses. The best known sources are in the mammalian stomach, yeast, and fungi, with porcine pepsin as the archetype, having been the first enzyme in this family to be sequenced and crystallized (1).

The aspartic proteinases are characterized by the presence of two aspartic acid residues at the active site. They tend to cleave between hydrophobic amino acids but secondary interactions are important in the definition of their specificity (2). The catalytic apparatus in all the aspartic proteinases is virtually the same and the differences among these enzymes are due mainly to the differences in specificity resulting from the structural evolution of the sites for substrate side chain binding. The hypothesis that the aspartic proteinases share the same catalytic apparatus is supported also by the fact that they are universally inhibited by pepstatin, a transition-state analogue inhibitor (3).

[1] To whom correspondence should be addressed.

Pepsin, an aspartic proteinase produced by the human gastric mucosa, can be found in seven different zymogen isoforms. These have been subdivided into two types: pepsinogen A (PGA1-5), and pepsinogen C (PGC6 and 7), both consist of molecular variants (isozymogens) that differ in net ionic charge (4). Pepsinogens are not secreted merely into the gastric lumen but also into the systemic circulation (5).

Pepsinogens A and C are translocated from the peptic cells into the circulation, and they are present in serum (6). However, only pepsinogen A can be found in urine by electrophoresis, indicating a different renal handling of pepsinogen A and pepsinogen C (5). Studies comparing the proteolytic activity of serum and urine have shown that the amount of pepsinogens in the urine correlate with the levels in serum. The concentration of pepsinogens in the urine, however, exceeds serum levels by about 10–100 times (7), which indicates a high clearance rate from the blood (5). The values of molecular weights of these proteins are around 40,000 Da for the zymogens, and about 35,000 Da for the active enzymes.

Various enzymes are known to be secreted into human urine as normal components. Changes of the activities of urinary enzymes are observed when our body conditions are physiologically abnormal (8). The urinary enzymes have not been studied in detail and should be characterized for their origin organs and tissues and their properties (9).

PGA and PGC are of medical interest as tumor markers. Low serum PGA levels are found in patients with atrophic gastritis or gastric cancer. Recent mass screening also revealed that serum PGA levels and PGA/PGC ratio are potentially useful parameters for the diagnosis of gastric cancer (10).

The properties of uropepsin obtained by activation of uropepsinogen were considered to be similar to those of human gastric pepsin. There is evidence that some amounts of the proenzyme produced in stomach tissue,

0006-291X/01 $35.00

come into the blood stream and finally into the urine, passing through the membranes of certain renal cells without undergoing any serious modifications (9).

Human pepsin consists of up to four isoforms of pepsinogen A with differing enzymatic properties. Uropepsin is one of these, which has the substitution Leu → Val at the position 291. This substitution will likely affect the specificity at S_3' and perhaps also at S_1' (11).

This article describes the modelling of the human uropepsin with pepstatin inhibitor. The investigation was made in order to gain further insight into the chemistry and functions of this protein.

MATERIALS AND METHODS

Purification of uropepsin. Human uropepsin has been extracted from urine of healthy young individuals without renal disease. The urine was stocked in bottles containing 6.0 M HCl solution. Five liters of this urine was filtered and dialyzed against distilled water. The solution was concentrated to the final volume of 50 ml and lyophilized. The uropepsin was purified using the same procedure described for human pepsin (12). Briefly, uropepsin purification was performed by a three-step procedure: DEAE Bio Gel (Bio Rad) chromatography, Mono Q 5/5 HR column (Pharmacia) chromatography (FPLC), and gel filtration (FPLC) on a Superdex 10/75 Column (Pharmacia).

Catalytic activity. Kinetic parameters were measured by the hydrolysis of a synthetic fluorogenic peptide containing at the extremities the chromophore *o*-aminobenzoyl (Abz) and its quenching partner *N*-(2,4-dinitrophenyl) ethylenediamine (Eddnp) which are separated by eight amino acid residues including two consecutive phenylalanine residues (13). Cleavage of the peptide between these hydrophobic residues results in a separation of the two peptide fragments, and a consequent dequenching of the Abz which leads to an increase in the fluorescence signal. Catalytic activity from pepsin 3A shown the value for K_m 1.53 ± 0.11 μM and k_{cat} 5.92 ± 0.21 s^{-1}. For uropepsin the value for K_m is 1.76 ± 0.09 μM and k_{cat} is 6.01 ± 0.11 s^{-1}, using the Abz-Lys-Pro-Ile-Glu-Phe-Phe-Arg-Leu-Eddnp as synthetic substrate in 0.2 M acetate buffer (pH 5.0). Concentrations of the substrate varied in the range 0.117–5.66 μM. K_{cat} values were calculated after titration of the active site with pepstatin.

Modelling. Several attempts of cocrystallizing the uropepsin with pepstatin did not produce crystals of high quality. A model of the uropepsin complex has been constructed. The model was based on the high-resolution crystal structure of pepsin complexed with pepstatin. Model building was carried out using model-by-homology of the program Modeller (14). The atomic coordinates for human pepsin complexed with pepstatin (PDB access code: 1PSO) solved by X-ray crystallography were used as a starting model. Torsion angles of the model were taken from the original structure whenever possible. Otherwise they were taken from a standard residue library. Where necessary the model was regularized. Reasonable positions for side chains that showed considerable Van der Waals overlap were obtained in an iterative process of flipping through all χ-angle rotamers. The pepstatin model was moved as a rigid body to approximately the same relative orientation of the pepstatin in the binary complex (1PSO), without any modification on the side chain positions of the pepstatin. The resulting crude structure was further optimized by means of variable target function method (VTFM) with conjugate gradient using Modeller.

Root-mean-square deviation (R.m.s.d.) differences from ideal geometries for bond lengths, angles, and dihedrals were calculated with X-PLOR 3.1 (15) and are presented in Table 1. The overall stereochemical quality of the final model for uropepsin was assessed by the program Procheck (16). Atomic models were superposed using the program LSQKAB from CCP4 (17).

TABLE 1

Root-Mean-Square Deviation (R.m.s.d.) Differences from Ideal Geometries

Observed deviation from ideal geometry	Uropepsin	Pepsin
Rms, bond lengths (Å)	0.005	0.008
Rms, bond angles (degrees)	1.23	1.79
Rms, impropers dihedrals (degrees)	2.84	4.28

RESULTS AND DISCUSSION

Quality of the Model

The overall stereochemical quality of the final model for the complex uropepsin:pepstatin was assessed by the program Procheck (16) and indicates that 100% of residues are in the allowed regions.

Overall Description

The model of the enzyme in the complex uropepsin: pepstatin is bilobal, consisting of two predominantly β-sheet lobes which, as observed in other aspartic proteinases, are related by pseudo twofold axis. The structure of human uropepsin follows closely the structure of porcine pepsin described previously (18). The uropepsin structure can be divided in three domains, analagous to the three domains of porcine pepsin (19). The central domain consists of a six-stranded antiparallel β-sheet that serves as a backbone to the active site region of the molecule. It is made up of residues Val1-Leu6, Asp149-Val184, and Glu308-Ala326. The N-terminal lobe is composed of residues Glu7-Gln148 and the C-terminal lobe is made up of residues Thr185-Arg307. The lobes consist of orthogonally packed β-sheets with the N- and C-terminal lobes having three and two layers, respectively.

We performed three superpositions: using all protein atoms (except for the atoms of the residue 291), using the main chain atoms (C, Cα, N, O), and α-carbons. The overall R.m.s.d. for superposition were 0.165 Å (all atoms), 0.146 Å (main chain atoms), and 0.103 Å (α-carbons).

Interactions with Pepstatin and Substrate-Binding Sites

It was observed that a total of 13 hydrogen bonds between uropepsin and pepstatin, most of them involving the catalytic aspartates (Asp32 and Asp215). The hydrogen bonding pattern between the inhibitor and the enzyme is well conserved in other structurally determined complexes with pepstatin (20). The distances of hydrogen bonding between Asp32 and Asp215 in

TABLE 2

Intermolecular Hydrogen Bonds of Pepsin and Uropepsin

Hydrogen bonds between active site and inhibitor		Distance (Å)	
Pepstatin	Enzyme	Uropepsin	Pepsin
Sta404 OH	Asp215 $O^{\delta 2}$	2.5	2.7
	Asp215 $O^{\delta 1}$	2.9	3.0
	Asp32 $O^{\delta 2}$	3.4	3.4
	Asp32 $O^{\delta 1}$	2.9	2.7
Sta404 N	Gly217 O	3.1	3.0
Sta404 OH	Gly217 O	*3.7*	3.5
Ala405 N	Gly34 O	*4.0*	2.9
Ala405 O	Tyr189 O^{η}	2.9	2.7
Val402 N	Ser219 O^{γ}	2.9	3.0
Val402 O	Ser219 N	3.0	3.0
Val403 N	Thr77 O^{γ}	2.8	3.1
Val403 O	Thr77 N	3.0	3.0
	Gly76 N	2.9	3.0
Sta404 O	Gly76 N	3.4	3.0
Sta406 N	Thr74 O	2.9	3.0

Note. Atoms which present distances larger than 3.5 Å were not considered as hydrogen bonded. Some of the distances are in italics, indicating that there are not hydrogens bonds in these positions in uropepsin. They are presented for comparison.

uropepsin and Sta404 in pepstatin are compatible with the pepsin complex, however the hydrogen bonding distances between Gly34-Ala405 and Gly217-Sta404 of the uropepsin and inhibitor are greater than those observed for the complex of pepsin:pepstatin (Table 2). As observed for crystallographic structures of complexes of inhibitors bound to aspartic proteinases, pepstatin in the modelled complex adopts an extended conformation with the first statyl hydroxyl oxygen occupying a position in the active site between the carboxyl groups of Asp32 and Asp215. The specificity and affinity between enzyme and its inhibitor depend on directional hydrogen bonds and ionic interactions, as well as on shape complementarity of the contact surfaces of both partners (21).

The electrostatic potential surface of the native uropepsin (PDB Accession code 1FLH) and the model complexed with pepstatin were calculated with GRASP (22). The same was performed with native and inhibited pepsin 3A. Two molecular surfaces were compared considering coordinates of the native and inhibited proteins. There is a conformational change in the structure when the inhibitor binds in the active site. The change is relatively small, with an R.m.s.d. difference in the coordinates of all the α-carbon atoms being 0.489 Å after superposition for pepsin 3 A and 0.850 Å for uropepsin. It can be clearly seen as a relative movement of the domains to enclose the inhibitor more closely in both binary complexes (Fig. 1).

We could observe that the overall structure of uropepsin and pepsin 3A are mostly negatively charged. The structures have few residues of histidine (1), lysine (0), and arginine (3). The active sites are strongly negative, as shown in Fig. 1. The contact surfaces for the binary complexes pepstatin:pepsin and pepstatin:uropepsin were calculated using Areaimol and Resarea (17), these contact areas show values of 348 and 601 $Å^2$, respectively.

The binding sites from S_4 to S_3' are defined by the interactions of the residues P_4 to P_3' of the inhibitor with the enzyme. It is unlikely that there are additional binding sites beyond these sites. The main-chain N of the P_3' residue forms a hydrogen bond to Thr 74. The S_4 pocket is flat and very accessible to solvent. The pockets S_1 and S_3 are contiguous, with the carbonyl O atom of Gly217 providing some separation of the two pockets. The S_1 pocket tends to be hydrophobic in nature, whereas the S_3 pocket is mainly polar. The S_2 and S_1' pockets are mainly hydrophobic. The S_2' pocket is clearly defined by the P_2' alanine residue (23).

The only difference in the primary sequence observed between pepsin 3A and uropepsin is the substitution Leu → Val in the position 291, located in S_3'

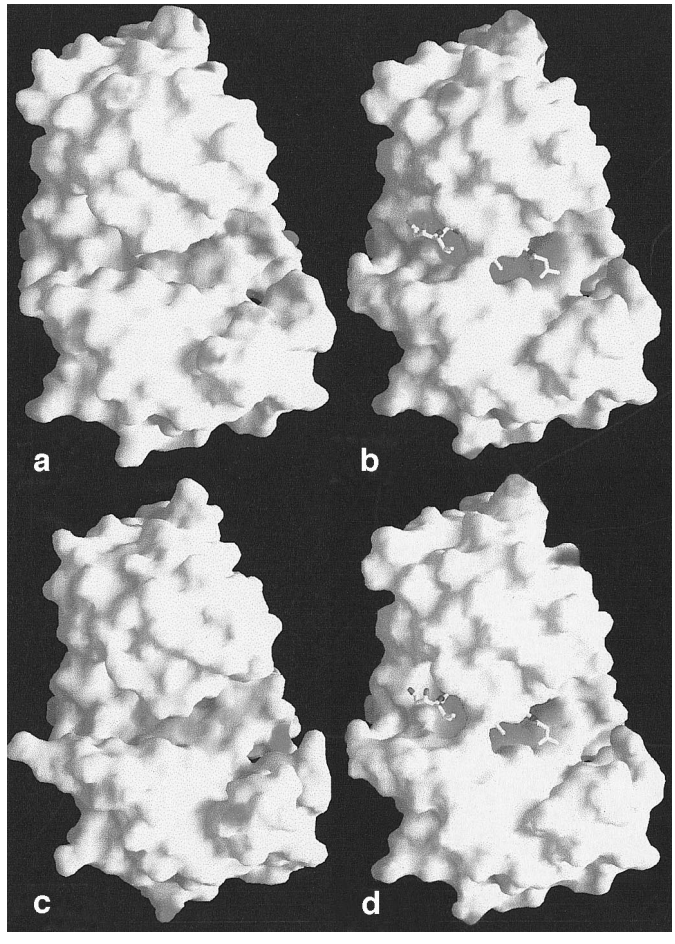

FIG. 1. Electrostatic potential surface of the pepsin (a) without inhibitor and (b) with inhibitor, and of the uropepsin (c) without inhibitor and (d) with inhibitor, calculated with GRASP (22), shown from −50 kT and +50 kT. Uncharged regions are in white.

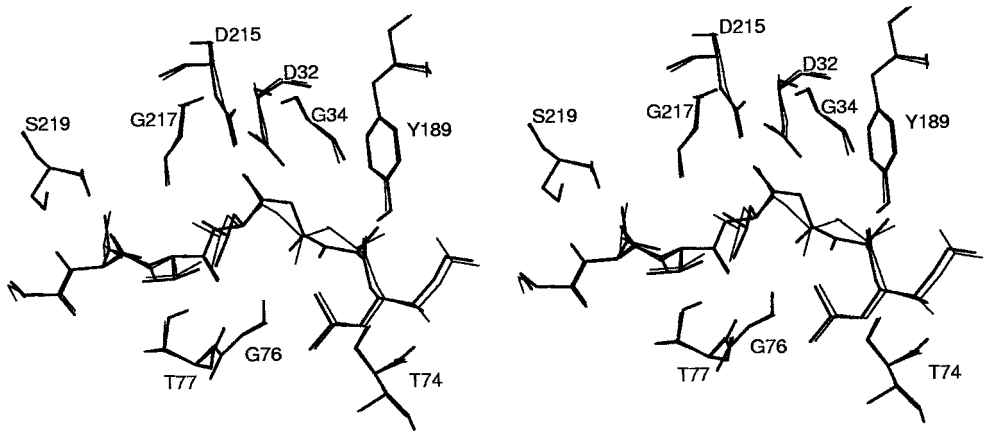

FIG. 2. Superimposed binding pockets of uropepsin:pepstatin complex (thick line) and pepsin:pepstatin complex (thin line).

pocket. It has been proposed that modifications on this pocket will likely affect the specificity at S_3' and perhaps also at S_1', which could affect the k_{cat} values for enzymes with mutations on this pocket (11). Nevertheless, it seems that this substitution on the binding pocket does not affect the k_{cat} values, since the values determined of k_{cat} for uropepsin and pepsin using the same substrate are $6.01 \pm 0.11\ s^{-1}$ and $5.92 \pm 0.21\ s^{-1}$, respectively. Furthermore, the substitution Leu → Val keeps the hydrophobicity in the S_3' pocket and the position adopted by the valine side chain does not affect the substrate binding.

The hydrogen bond between Gly34-Ala405 and Gly217-Sta404 observed for the pepsin:pepstatin complex are not maintained for the complex uropepsin: pepstatin (Table 2). However, a close examination of the binary complexes pepsin:pepstatin and uropepsin: pepstatin shows clearly that the inhibitor adopts the same orientation in both complexes (Fig. 2). Furthermore the hydrogen bonds between Asp32 and Asp215 and the inhibitor are conserved in both complexes. Table 3 shows a comparison of structural and activity parameters between pepsin and uropepsin. The major structural difference between the two binary complexes is observed for the contact area between the enzymes and pepstatin. This difference is probably due to differences in the S3′ pocket, however most of the structural parameters for these two complexes present close values. This structural similarity confirms the activity similarity against pepstatin observed between the two enzymes which strongly indicates that the modifications on S3′ pocket of aspartic proteinases have litle effect on the k_{cat} and on the three-dimensional structure of these class of enzymes.

TABLE 3

Structural and Activity Parameters for Uropepsin and Pepsin

Parameters	Pepsin	Uropepsin
Solvent accessible surface (Å^2)	12587	13481
Contact surface between enzyme and pepstatin (Å^2)	348	601
Number of hydrogen bonds between enzyme and pepstatin	15	13
Main residues involved on the contact with pepstatin	Asp32 Asp215	Asp32 Asp215
k_{cat} (s^{-1})	5.92 ± 0.21	6.01 ± 0.11
k_m (μM)	1.53 ± 0.11	1.76 ± 0.09

ACKNOWLEDGMENTS

We thank Andressa Salbé dos Santos Oliveira for the English revision. This work was supported by grants from FAPESP, CNPq, CAPES, and Fundo Bunka de Pesquisa (Banco Sumitomo). W.F.A. Jr. is a researcher for the Brazilian Council for Scientific and Technological Development (CNPq, 300851/98-7).

REFERENCES

1. Szecsi, P. B. (1992) The aspartic proteinases. *Scand. J. Clin. Lab. Invest.* **52**(Suppl. 210), 5–22.
2. Powers, J. C., Harley, A. D., and Myers, D. V. (1977) Subsite specificity of porcine pepsin. *In* Acid Proteinases, Structure, Function & Biology (Tang, J., Ed.), pp. 141–157, Plenum, NY.
3. Marciniszyn, J., Jr., Hartsuck, J. A., and Tang, J. (1976) Mode of inhibition of acid proteases by pepstatin. *J. Biol. Chem.* **251,** 7088–7094.
4. Foltmann, B. (1981) Gastric proteinases—Structure, function, evolution and mechanism of action. *Essays in Biochem.* **17,** 52–84.
5. Samloff, I. M., and Taggart, R. T. (1987) Pepsinogens, pepsins, and peptic ulcer. *Clin. Invest. Med.* **10**(3), 215–221.
6. Ten Kate, R. W., Pals, G., Pronk, J. C., Bank, R. A., Eriksson, A. W., Donker, A. B. J. M., and Meuwissen, S. G. M. (1988) Renal handling of pepsinogen A and C in man. *Clinical Science* **75,** 649–654.
7. Samloff, I. M., and Townes, P. L. (1970) Electrophoretic heterogeneity and relationships of pepsinogens in human urine, serum, and gastric mucosa. *Gastroenterology* **58,** 462–469.

8. Rabb, W. P. (1972) Diagnostic value of urinary enzyme determinations. *Clinical Chemistry* **18**(1), 5–25.
9. Minamiura, N., Ito, K., Kobayashi, M., Kobayashi, O., and Yamamoto, T. (1984) Uropepsinogen in human urine: Its protein nature, activation and enzymatic properties of activated enzyme. *J. Biochem.* **96,** 1061–1069.
10. Hattori, Y., Tashiro, H., Kawamoto, T., and Kodama, Y. (1995) Sensitivity and specificity of mass screening for gastric cancer using the measurement of serum pepsinogens. *Jpn. J. Cancer Res.* **86,** 1210–1215.
11. Fujinaga, M., Chernaia, M. M., Tarasova, N. I., Mosimann, S. C., and James, M. N. G. (1995) Crystal structure of human pepsin and its complex with pepstatin. *Protein Sci.* **4,** 960–972.
12. Gomes, R. A. S., Chagas, J. R., Juliano, L., and Hial, V. (1996) Met-Lys-Bradykinin-Ser, the kinin released from human kininogen by human pepsin. *Immunopharmacology* **32,** 76–79.
13. Filippova, I. Yu., Lysogorskaya, E. N., Anisimova, V. V., Suvorov, L. I., Oksenoit, E. S., and Stepanov, V. M. (1996) Fluorogenic peptide substrates for assay of aspartic proteinases. *Anal. Biochem.* **234,** 113–118.
14. Šali, A., and Blundell, T. L. (1993) Comparative protein modelling by satisfaction of spatial restraints. *J. Mol. Biol.* **234,** 779–815.
15. Brünger, A. T. (1992) X-PLOR Version 3.1: A system for crystallography and NMR. Yale University Press, New Haven.
16. Laskowski, R. A., MacArthur, M. W., Moss, D. S., and Thornton, J. M. (1993) Procheck: A program to check the stereochemical quality of protein structures. *J. Appl. Cryst.* **26,** 283–291.
17. CCP4 (1994) The CCP4 Suite: Programs for Protein Crystallography. *Acta Cryst.* **D50,** 760–763.
18. Cooper, J. B., Khan, G., Taylor, G., Tickle, I. J., and Blundell, T. L. (1990) X-ray analyses of aspartic proteinases: II. Three-dimensional structure of the hexagonal crystal form of porcine pepsin at 2.3 Å resolution. *J. Mol. Biol.* **214,** 199–222.
19. Sielecki, A. R., Fedorov, A. A., Boodhoo, A., Andreeva, N. S., and James, M. N. G. (1990) Molecular and crystal structures of monoclinic porcine pepsin refined at 1.8 Å resolution. *J. Mol. Biol.* **214,** 143–170.
20. Baldwin, E. T., Bhat, T. N., Gulnik, S., Hosur, M. V., Sowder, R. C., II, Cachau, R. E., Collins, J., Silva, A. M., and Erickson, J. W. (1993) Crystal structures of native and inhibited forms of human cathepsin D: Implications for lysosomal targeting and drug design. *Proc. Natl. Acad. Sci. USA* **90,** 6796–6800.
21. de Azevedo, W. F., Jr., Leclerc, S., Meijer, L., Havlicek, L., Strnad, M., and Kim, S.-H. (1997) Inhibition of cyclin-dependent kinases by purine analogues: Crystal structure of human CDK2 complexed with roscovitine. *Eur. J. Biochemistry* **243,** 518–526.
22. Nicholls, A., Sharp, K., and Honig, B. (1991) Protein folding and association: Insights from the interfacial and thermodynamic properties of hydrocarbons. *Proteins Struct. Funct. Genet.* **11,** 281.
23. Fujinaga, M., Cherney, M. M., Tarasova, N. I., Bartlett, P. A., Hanson, J. E., and James, M. N. G. (2000) Structural study of the complex between human pepsin and a phosphorus-containing peptidic transition-state analog. *Acta Cryst.* **D56,** 272–279.